An Extended Approach to UAV Parameter Estimation using Simulated Flight Data

Stephen Kimathi[1,2], **Bela Lantos**[1]

[1]Department of Control Engineering and Information Technology, Budapest University of Technology and Economics, Magyar tudósok krt. 2, H-1117 Budapest, Hungary

[2]Department of Electrical and Electronic Engineering, Dedan Kimathi University of Technology, Private Bag-10143, Dedan Kimathi, Nyeri, Kenya

e-mail: kimathi@iit.bme.hu, lantos@iit.bme.hu

Abstract: Parameter estimation of aircraft aerodynamic coefficients from experimental flight data generated using dynamics of postulated equations of motion describing the aerodynamics model is presented. Since the dynamics are characterized by aerodynamic and control derivatives, then these parameters can be extracted from the flight data. The one shot least squares method based on the equation error is used to estimate the initial parameters. The response outputs of the model estimate form the basis that an update of the model parameters is sought through the use of inversing modelling, and the output error method. Model validation metrics based on statistical analysis of the parameter estimates are then used to evaluate the degree of model fit, and the predictive capability of the identified model.

Keywords: Parameter estimation; least squares; output-error; inverse model; YAK-54

1 Introduction

For a specified model, system identification amounts to determining the model parameters θ, such that the model estimate response $\hat{y}$, matches adequately to the system response z. This process is commonly referred to as parameter estimation, such that the unknown model parameters are determined indirectly from the system's measured data. In essence, a model estimate should sufficiently capture the underlying features and dependencies in the measured data, while also strife for simplicity. Therefore, simplified representations are realized from the complex nonlinear behaviours of the physical models through system identification. To assess the adequacy of the model parameter estimates, model validation is usually carried out.

When system identification is applied to an aerial vehicle, the equations of motion governing an aircraft dynamic response are usually postulated, and an experiment

is designed to obtain measurements through excitation of the inputs to the system. Different types of excitation inputs exist for aerial vehicles including multistep inputs [1], frequency sweeps [2] [3], multisines [4] [5], and pilot controls. For other applications chirps and pseudorandom signals [6] can also be applied. However, if the input waveforms to the different input channels have a similar appearance, then it becomes impossible to determine which input moved in a certain manner to contribute to the change(s) in the aerodynamic forces and moments. Hence, any process that tries to assign values to the model parameters using such inputs might fail to extract the correct relationships [7]. Optimal inputs have been suggested and used in [8], however, since the objective is to identify the model parameters, designing optimal inputs usually involve a large computation time, and thus superfluous. It has been shown that designing orthogonal input waveforms improve system excitation, and results in uncorrelated inputs [2].

System identification of dynamic models from their response data is motivated by the ability to use the resulting models that mimic the behaviour of the system as closely as possible as a foundation for purposes of control synthesis or motion planning. Different types of response data have been used for system identification such as flight data in [9], computational fluid dynamics data in [10], wind tunnel data in [11], and simulation flight data in [12]. A candidate method including equation error [13], filter error [14], output error [15], or neural networks [16] is then applied to estimate aerodynamic model parameters from the response data. These methods seek to minimize the squared differences between the observations and predicted value.

In this work, the equation error method is applied, and an extra update step is done based on the output errors from the computed responses through the use of inverse simulation, so as to improve the convergence of the model parameters. This is important especially when the aerodynamic force and moment reconstruction is desired such as during control reconfiguration [17].

This paper is structured as follows: Section 2 describes formulation of the aerodynamic model of an unmanned aerial vehicle (UAV). Section 3 presents some principles of system identification, and the test data used in the identification of the model parameters is discussed in Section 4. The estimation of the parameters from the test data is presented in Section 5, and thereafter the conclusion is given.

2 UAV Aerodynamic Model Formulation

Let's denote $(u,v,w)^T$ and $(p,q,r)^T$ to represent the velocity and angular velocity components respectively in the body frame's center of gravity. The force and moment equations of a UAV expressed in the body frame can then be expressed by (1-2).

$$\left.\begin{aligned} F_x &= m(\dot{u} + qw - rv) \\ F_y &= m(\dot{v} + ru - pw) \\ F_z &= m(\dot{w} + pv - qu) \end{aligned}\right\} \tag{1}$$

$$\left.\begin{aligned} M_x &= \dot{p}I_x - \dot{r}I_{xz} + qr(I_z - I_y) - qpI_{xz} \\ M_y &= \dot{q}I_y + pr(I_x - I_z) + (p^2 - r^2)I_{xz} \\ M_z &= \dot{r}I_z - \dot{p}I_{xz} + pq(I_y - I_x) + qrI_{xz} \end{aligned}\right\} \tag{2}$$

$F_{x,y,z}$ and $M_{x,y,z}$ are composed of contribution from aerodynamics, thrust and gravity as expressed in (3-4).

$$F_{x,y,z} = F_{aero} + F_g + F_T = \bar{q}S\begin{bmatrix} C_x \\ C_y \\ C_z \end{bmatrix} + \begin{bmatrix} -mg\sin\theta \\ mg\sin\phi\cos\theta \\ mg\cos\phi\cos\theta \end{bmatrix} + \begin{bmatrix} T \\ 0 \\ 0 \end{bmatrix} \tag{3}$$

$$M_{x,y,z} = M_{aero} = \bar{q}S\begin{bmatrix} bC_l \\ \bar{c}C_m \\ bC_n \end{bmatrix} \tag{4}$$

where $\bar{q} = \frac{1}{2}\rho V^2$ is the dynamic pressure, and the variables $S, \rho, b, \bar{c}, S, I_*$ have their usual meaning according to aircraft literature [7] [18]. The force and moment equations become (5-6) after substituting (3-4) into (1-2).

$$\begin{aligned} \dot{u} &= \left[m(rv - qw) + \bar{q}SC_x - mg\sin\theta + T\right]/m \\ \dot{v} &= \left[m(pw - ru) + \bar{q}SC_y + mg\sin\phi\cos\theta\right]/m \\ \dot{w} &= \left[m(qu - pv) + \bar{q}SC_z + mg\cos\phi\cos\theta\right]/m \end{aligned} \tag{5}$$

$$\begin{aligned} \dot{p}I_x - \dot{r}I_{xz} &= qr(I_y - I_z) + qpI_{xz} + \bar{q}SbC_l \\ \dot{q}I_y &= pr(I_z - I_x) + (r^2 - p^2)I_{xz} + \bar{q}S\bar{c}C_m \\ \dot{r}I_z - \dot{p}I_{xz} &= pq(I_x - I_y) - qrI_{xz} + \bar{q}SbC_n \end{aligned} \tag{6}$$

The force equation (5) is transformed to wind axis, and expressed in terms of airspeed V, angle of attack α, and side slip angle β to become (7).

$$\begin{aligned} \dot{V} &= -\frac{\bar{q}S}{m}C_{D_W} + \frac{T}{m}C_\alpha C_\beta + gW_1 \\ \dot{\beta} &= \frac{\bar{q}S}{mV}C_{Y_W} + \Gamma_1 - \frac{T}{mV}C_\alpha S_\beta + \frac{gW_2}{V} \\ \dot{\alpha} &= -\frac{\bar{q}S}{mVC_\beta}C_L + q - \Gamma_2 - \frac{T}{mVC_\beta}S_\alpha + \frac{gW3}{VC_\beta} \end{aligned} \tag{7}$$

where $C_\alpha = \cos(\alpha)$, $C_\beta = \cos(\beta)$, $S_\alpha = \sin(\alpha)$, $S_\beta = \sin(\beta)$ and $T_\beta = \tan(\beta)$. $C_{D_W} = C_D C_\beta - C_Y S_\beta$, $C_{Y_W} = C_Y C_\beta + C_D S_\beta$, $\Gamma_1 = pS_\alpha - rC_\alpha$, $\Gamma_2 = T_\beta(pC_\alpha + rS_\alpha)$ and (gW_1, gW_2, gW_3) are the gravity acceleration components in the wind axis frame. Equation (6) and (7) are the equations of motion and are developed with the assumption that an aircraft is a rigid body, and its thrust acts along the x-axis through the aircraft center of gravity. For quasi steady flow, the functional form of the non-dimensional force and moment aerodynamic coefficients are expressed as $C_* = C_*(\alpha, \beta, \hat{p}, \hat{q}, \hat{r}, \delta_s)$, where $* \Rightarrow D, Y, L, l, m, n$, and δ_s represent aircraft controls of aileron, elevator and rudder. The variables and parameters of the equation of motions (6-7) are listed in Table 1.

Table 1
Summary of one-shot least squares parameters

Coefficient	**Observation, Y**	**Regressors, X**	**Parameters, θ**
Drag	C_D	$1, \alpha$	$C_{D0}, C_{D\alpha}$
Side-force	C_Y	$\beta, \hat{p}, \hat{r}, \delta_a, \delta_r$	$C_{Y\beta}, C_{Yp}, C_{Yr}, C_{Y\delta_a}, C_{Y\delta_r}$
Lift	C_L	$1, \alpha, \hat{q}, \delta_e$	$C_{L0}, C_{L\alpha}, C_{Lq}, C_{L\delta_e}$
Rolling moment	C_l	$\beta, \hat{p}, \hat{r}, \delta_a, \delta_r$	$C_{l\beta}, C_{lp}, C_{lr}, C_{l\delta_a}, C_{l\delta_r}$
Pitching moment	C_m	$1, \alpha, \hat{q}, \delta_e$	$C_{m0}, C_{m\alpha}, C_{mq}, C_{m\delta_e}$
Yawing moment	C_n	$\beta, \hat{p}, \hat{r}, \delta_a, \delta_r$	$C_{n\beta}, C_{np}, C_{nr}, C_{n\delta_a}, C_{n\delta_r}$

where $(\hat{p}, \hat{q}, \hat{r}) = \left(\frac{b}{2V_a} p, \frac{c}{2V_a} q, \frac{b}{2V_a} r \right)$. The structure for the identification model culminates to the solution of the unknown parameters θ_j, $j = 1, 2, \ldots n_p$ representing the aerodynamic coefficients. Reorganizing (6-7) result into (8) where the right side of together with the relations in (7) are the observations, and the left side form the regressors for the parameter estimation process.

$$
\begin{aligned}
C_{D_W} &= \left(-m\dot{V} + TC_\alpha C_\beta + mgW_1\right) / \bar{q}S \\
C_{Y_W} &= \left(mV\left[\dot{\beta} - \Gamma_1\right] + TC_\alpha S_\beta - gW_2\right) / \bar{q}S \\
C_L &= \left(mVC_\beta\left[-\dot{\alpha} + q - \Gamma_2\right] - TS_\alpha + mgW_3\right) / \bar{q}S \\
C_l &= \left(\dot{p}I_x + qr(I_z - I_y) - (qp + \dot{r})I_{xz}\right) / \bar{q}Sb \\
C_m &= \left(\dot{q}I_y + pr(I_x - I_z) + (p^2 - r^2)I_{xz}\right) / \bar{q}S\bar{c} \\
C_n &= \left(\dot{r}I_z + pq(I_y - I_x) + (qr - \dot{p}I_{xz})I_{xz}\right) / \bar{q}Sb
\end{aligned}
\tag{8}
$$

3 System Identification

The objective when conducting flight tests for system identification, is to excite all the dynamic modes of an aircraft. In order to obtain to a good model estimate, the excitation to the system must be sufficient enough to stimulate the natural dynamic response in the aircraft motion. The excitation is normally fed in as an input into the input channels of the system.

3.1 Input Design

Orthogonal input waveforms are the desired excitation in this work. Multisines which are a sum of sinusoids with varying amplitudes, frequencies and phase angles are used. The frequencies for the multisines are normally chosen to cover a frequency band of interest, while the phase angles can be chosen arbitrarily [7]. A multisine takes the form

$$u(i) = \sum_{k=1}^{M} A_k \cos\left(\frac{2\pi k t(i)}{T} + \phi_k\right), \qquad i = 0,1,2,\ldots,N-1 \tag{9}$$

where M is the total number of available harmonically related frequencies, T is the time length of the excitation, and ϕ_k are phase angles for each of the harmonic components. For Schroeder sweeps, $A_k = \sqrt{P/M}$, and

$$\phi_k = \phi_{k-1} - \pi k^2/M, \qquad k = 2,3,\ldots M \tag{10}$$

where P is the total desired input power. Multisines using phase angles in (10) result in inputs with low relative peak factors, RPF. However, these inputs do not qualify as perturbation inputs, that is, that of starting and ending at zero [4]. The initial phase angle(s) ϕ_1 can be adjusted accordingly, and thus satisfy the perturbation requirement. The process of designing orthogonal multisine inputs is:

a) Assign an appropriate equal number of indices k to each input from a set $K = \{1,2,\ldots M\}$. Each frequency index can only be assigned to only one input. For instance, each input can consist of an integer in K and multiples of that integer.

b) The desired input power is then defined, ideally it should be constant for all the inputs. This is a generalization, but still sufficient to excite the aircraft dynamics. If need be, optimization of the frequency spectrum of inputs can be done.

c) Generate the input $u(i)$ for each of the m excitation input, using (9).

d) Using a one-dimensional search, find the phase shift to be added to each component such that each input $u(i)$, appears as a perturbation input.

It is postulated in [4], that signals designed in this manner will be orthogonal in the time-domain regardless of the individual phase shifts. Hence, inputs composed of signals in this form will be decorrelated, and thus give accurate input control effectiveness on a system.

3.2 Equation-Error Method

Denote $y(k) = x(k)\theta$ as the linear hypothesis about the parameter dependence. The equation-error method based on least squares, LS is simple, powerful, and sufficiently captures the underlying dependencies in any observation data. Consider the following equation

$$z(k) = x^T(k)\theta + \varepsilon(k), \qquad k = 1,\ldots,N \tag{11}$$

where $\theta = (1,\theta_2 \ldots,\theta_{n_p})^T$ represent the unknown parameters, z represent the observation, and x represent the independent variables also called regressors. ε is the uncorrelated error representing residuals. θ is assumed constant over all N data samples. For the N data points, (11) become $Z = X\theta + \mathrm{E}$, where Z, E, and X are $N \times 1$, $N \times 1$ and $N \times n_p$ matrices respectively. The least squares parameter estimates $\hat{\theta}$ of the true value θ is given by:

$$\hat{\theta} = (X^T X)^{-1} X^T Z. \tag{12}$$

For a complete derivation of (12), see [19]. Singular value decomposition or Cholesky factorization can be used to compute the term $(X^T X)^{-1}$, and if it exists, then $\hat{\theta}$ will be unique.

3.3 Output-Error Method

Consider system dynamics described by $\dot{x} = f(x,u,\theta)$, and $y = g(x,u,\theta)$. Since it is not possible to measure the system parameters θ, they can be estimated from the measurements $z(k)$ of the model response outputs $y(k)$ at discrete points k. The output equation is rewritten as:

$$z(k) = y(k) + v(k) \tag{13}$$

where $v(k)$ are the output measurement errors with $E(v) = 0$, and $E(vv^T) = \mathbf{R}$.

The output-error is a maximum likelihood method, and therefore for a given $\mathbf{R}$, optimizing a negative log-likelihood cost function result in optimizing the function $J(\theta)$ that is subject to the model parameters using the covariance matrix estimate $\hat{\mathbf{R}}$.

$$J(\theta)=\frac{1}{2}\sum_{k=1}^{N}v(k)\hat{\mathbf{R}}^{-1}v^{T}(k),\qquad \hat{\mathbf{R}}=diag\left(\frac{1}{N}\sum_{k=1}^{N}v(k)v^{T}(k)\right) \tag{14}$$

Taking the gradient and the second order gradient of the cost function $J(\theta)$, results to (15-16).

$$\frac{\partial J(\theta)}{\partial \theta_j}=\mathbf{S}(k)=-\sum_{k=1}^{N}\frac{\partial y^{T}(k)}{\partial \theta_j}\hat{\mathbf{R}}^{-1}v(k)\qquad j=1,...n_p \tag{15}$$

$$\frac{\partial^2 J(\theta)}{\partial \theta_j\theta_i}=\sum_{k=1}^{N}\frac{\partial y^{T}(k)}{\partial \theta_j}\hat{\mathbf{R}}^{-1}\frac{\partial y(k)}{\partial \theta_i}-\sum_{k=1}^{N}\frac{\partial^2 y^{T}(k)}{\partial \theta_j\theta_i}\hat{\mathbf{R}}^{-1}v(k)\qquad j,i=1,...n_p \tag{16}$$

The higher orders of the partial derivatives in (16) are normally ignored [7] for practical reasons, resulting in a simplified Fisher information matrix, $F=\partial^2 J(\theta)/\partial\theta_j\theta_i$. The maximum likelihood parameter estimator in its general form is the given as:

$$\hat{\theta}_{i+1}=\theta_i-\Delta\theta \tag{17}$$

where $\Delta\theta=F^{-1}\mathbf{S}(k)$ and $Cov(\hat{\theta})\geq F^{-1}$. The relaxation technique is then applied such that the covariance $\hat{\mathbf{R}}$ is first computed, then the cost gradient and information matrix, and finally the parameter update is carried out using (17).

3.4 Model Validation of Aircraft Parameter Estimates

After parameters of a model have been estimated, an investigation of the parameter's correctness and adequacy in the model estimate should be done. This can be achieved by checking the polarity of the estimates from a theoretical background. Moreover, a coefficient of determination (18) can give insights about the model estimates' ability to predict the measured data, where a value 1 represents a perfect fit to the data [7].

$$R^2=\frac{\hat{\theta}^{T}X^{T}z-N\bar{z}^2}{z^{T}z-N\bar{z}^2},\left\{R^2\in[0,1]\right\} \tag{18}$$

Different techniques are usually required to evaluate the adequacy of updated model parameters in a model estimate. The easiest way to compare two competing models is to measure how well each model performs reclassification. Reclassification for instance, may entail comparing the responses of the actual against the predicted outputs of the different models.

4 Flight Tests

In system identification experiments, real flight data in most cases is not readily available or that, which is available does not include flight profiles necessary for system identification. In such scenarios, simulated flight data provide a good alternative [16]. A flight test was executed to generate test data from which a model estimate could be extracted. The excitation for the three input control signals $(\delta_a, \delta_e, \delta_r)$ were designed using multisines where the parameters of (9-10) are given in Table 2. The ensuing signals are shown in Fig. 1.

Table 2
Multi-input design parameters

Input	k	RPF
Aileron, δ_a	3,6,12	1.2318
Elevator, δ_e	2,4,8	1.4451
Rudder, δ_r	5,10,15	1.2679

Equations (6-7) were used to carry out numerical simulations in Matlab using the YAK-54 unmanned aircraft airframe physical properties as listed in [20]. The input signals were applied simultaneously since this is a more efficient way for exciting the dynamic modes of a system instead of moving them separately [21].

Due to the nature of inputs signals which might be misconstrued as a disturbance in a feedback control system, and hence the dynamic response of the aircraft subdued, an open loop simulation configuration was used. The flight data from the numerical simulation is shown in Fig. 2.

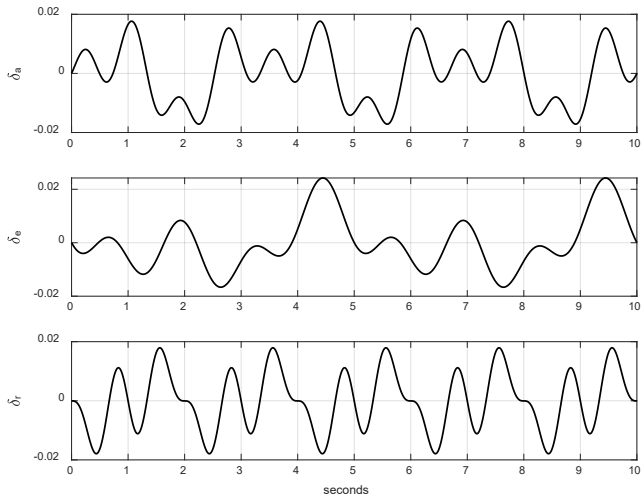

Figure 1
Excitation inputs to the system

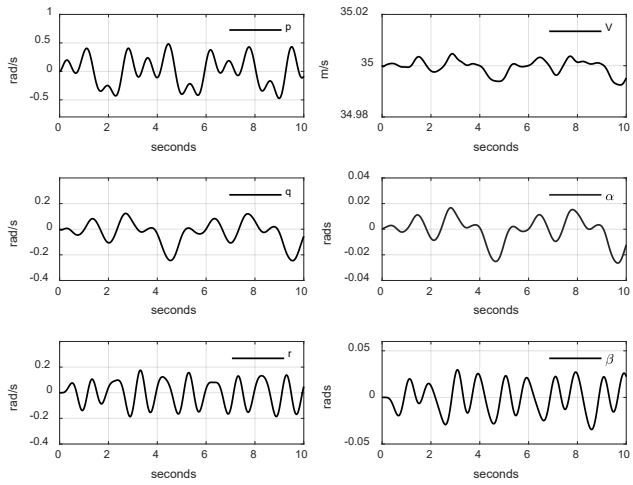

Figure 2
System identification data

5 Parameter Estimation Results

5.1 Initial Parameter Estimates

To estimate the parameters of the aerodynamic model listed in Table 1, the equation error method discussed in Sec. 3.2 was used. The regressors were computed using (8) and the test data in Fig. 2. Table 3 and Table 4 show the force and moment parameter estimates respectively and their standard deviations. The coefficient of determination calculated using (18) was 89.23%, which represents the percentage proportion in the variation of the measured output that is explained by the identified model.

Table 3
Parameter estimates of the force coefficients

Coeff.	θ	$\hat{\theta}_{LS}$	$s(\hat{\theta}_{LS})\times 10^{-2}$	**Coeff.**	θ	$\hat{\theta}_{LS}$	$s(\hat{\theta}_{LS})\times 10^{-2}$
C_{D0}	0.0526	0.0536	0.0019	C_{L0}	0.1470	0.1453	0.0019
$C_{D\alpha}$	-0.0863	-0.0889	0.0080	$C_{L\alpha}$	4.5363	4.6505	0.2528
$C_{Y\beta}$	-0.3462	-0.4761	0.2276	C_{Lq}	5.1515	4.5196	0.8871
C_{Yp}	0.0073	0.0164	0.2285	$C_{L\delta_e}$	0.3762	0.5502	0.3054
C_{Yr}	0.2372	0.1994	0.5526	$C_{Y\delta_r}$	0.1928	0.0784	0.2620

Table 4
Parameter estimates for the moment coefficients

Coeff.	θ	$\hat{\theta}_{LS}$	$s(\hat{\theta}_{LS})\times10^{-3}$	**Coeff.**	θ	$\hat{\theta}_{LS}$	$s(\hat{\theta}_{LS})\times10^{-3}$
$C_{l\beta}$	-0.0255	-0.0232	0.0080	C_{mq}	-8.5026	-6.5773	2.11
C_{lp}	-0.3817	-0.3403	0.0467	$C_{m\delta_e}$	-0.8778	-0.7974	0.0755
C_{lr}	0.0504	0.0472	0.0406	$C_{n\beta}$	0.0954	0.0942	0.0101
$C_{l\delta_a}$	0.3490	0.3150	0.0377	C_{np}	-0.0156	-0.0157	0.0778
$C_{l\delta_r}$	0.0154	0.0140	0.0170	C_{nr}	-0.1161	-0.0913	0.0440
C_{m0}	-0.0018	-0.0015	0.0002	$C_{n\delta_a}$	-0.0088	-0.0083	0.0724
$C_{m\alpha}$	-0.3701	-0.3931	0.0066	$C_{n\delta_r}$	-0.0996	-0.0978	0.0173

The model response outputs using the measured response control inputs and the estimated model parameters was compared with the measured response data. A plot of the forces and moments from the estimated model are given in Figs. 3 and 4 respectively.

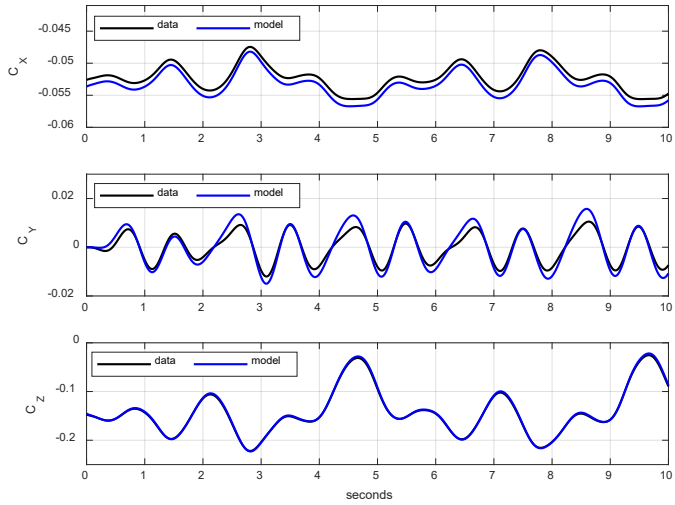

Figure 3
Model fit to force coefficients

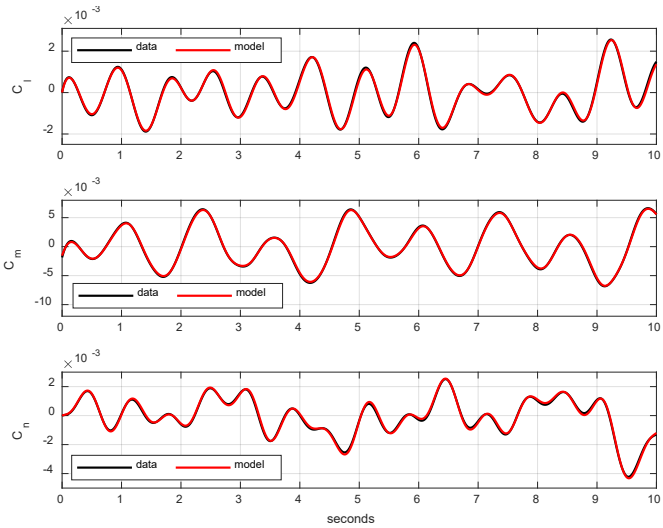

Figure 4
Model fit to moment coefficients

It can be seen that the moment plots have a perfect fit to the data. The forces plots show a good fit only in the normal force, C_Z. A close inspection reveals that a big portion of the difference in the response of C_X is attributable to the difference in the bias parameter, C_{D0} while in C_Y, the deviation might be attributable to the magnitudes of the parameters. The root mean squared error [7], RMSE values of the model prediction are given in Table 5.

Table 5
RMSE values

Variable	RMSE	Variable	RMSE
C_X	0.0178	C_l	3.8×10^{-5}
C_Y	0.0036	C_m	7.45×10^{-5}
C_Z	0.0012	C_n	4.86×10^{-5}

5.2 Adjustment of the Initial Estimates

The difference between the model estimates response outputs and the measured response data was computed and is shown in Fig. 5. These deviations contain the model deficiencies. A suitable metric to assess these deficiencies is that they should be small and oscillate about zero, otherwise, they present possible clues for model updates or extensions [19]. The measured response data is used as the reference, and an inverse simulation [22] using nonlinear dynamic inversion was carried out to determine the required time histories of the control inputs and state

variables to compensate for the model deficiencies. The desired input time histories from this processing are shown in Fig. 6.

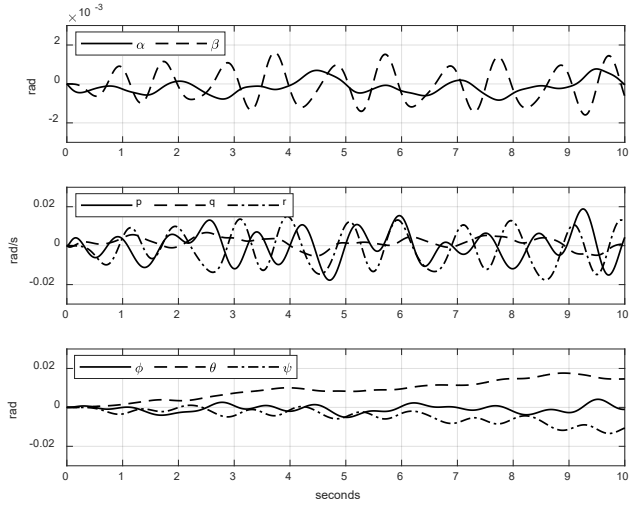

Figure 5
Deviations of response in output variables

The output-error method using these time histories was the applied to update the force model parameter estimates using (17) with the identified estimates as the initial values. The concept behind this, is that of establishing consistent dynamic characteristics in the forces and moments. Table 6 lists the updated parameter estimates, $\hat{\theta}^*$ alongside the initial estimates, $\hat{\theta}$ and the percentage errors.

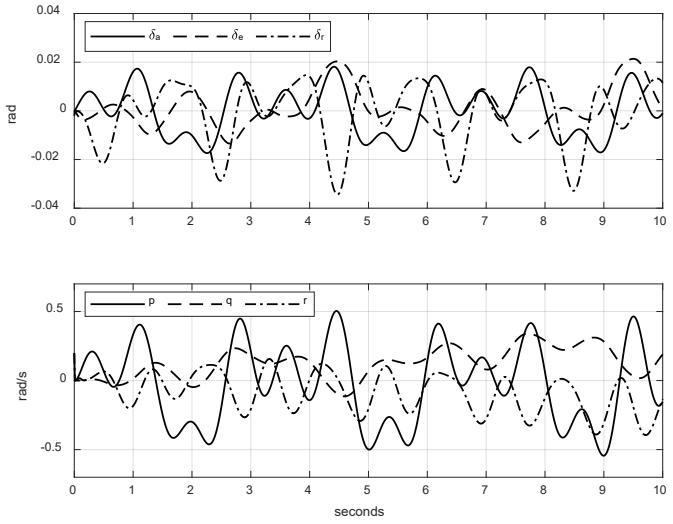

Figure 6
Desired input and angular rates time histories

Table 6
Updated force parameter estimates

Parameter	θ	$\hat{\theta}$	% Error	$\hat{\theta}^*$	% Error
C_{D0}	0.0526	0.0536	1.9	0.0526	0
$C_{D\alpha}$	-0.0863	-0.0889	4.17	-0.0835	3.2
$C_{Y\beta}$	-0.3462	-0.4761	37.52	-0.3949	14.07
C_{Yp}	0.0073	0.0164	124.66	0.0140	91.78
C_{Yr}	0.2372	0.1994	15.94	0.2188	7.75
$C_{Y\delta_r}$	0.1928	0.0784	59.34	0.1723	10.63
C_{L0}	0.1470	0.1453	1.15	0.1461	0.61
$C_{L\alpha}$	4.5363	4.6505	2.52	4.5524	0.35
C_{Lq}	5.1515	4.5196	12.27	4.7409	7.97
$C_{L\delta_e}$	0.3762	0.5502	46.25	0.5482	45.72

It can be seen that, there was asymptotic improvements in all the coefficients towards convergence. A model fit graph based on the updated force parameter estimates are shown in Fig. 7. The individual graphs show improved fits as compared to initial estimated model fits in Fig. 3. In the axial force C_X, the bias term is accurately compensated and hence a robust fit. The side force C_Y, also show an improved fit, with the overshoots greatly reduced.

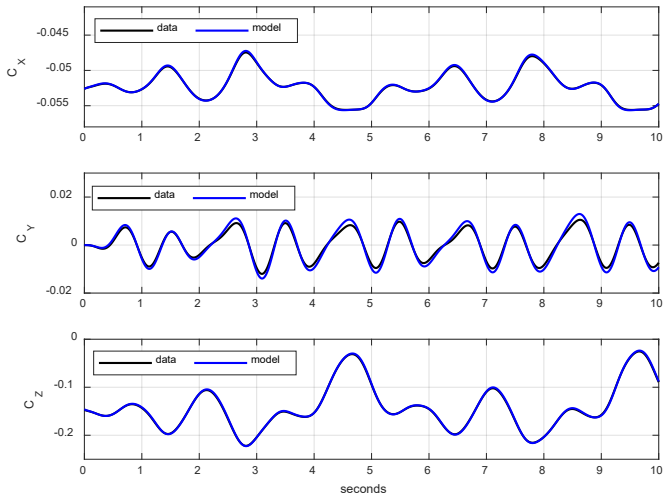

Figure 7
Model fit of force coefficients after update

Finally, a side-by-side comparison of the model estimates using the approach discussed here and that presented in [20] was done. These two identification models have a similar model structure and parameterization of the model parameters.

The model parameters are listed in Table 7, where the parameters identified using the approach in this work, are labelled $\hat{\theta}_2$, and from that other approach as $\hat{\theta}_1$.

Table 7
Comparison of force and moment model parameters

Coeff.	θ	$\hat{\theta}_1$	$\hat{\theta}_2$	**Coeff.**	θ	$\hat{\theta}_1$	$\hat{\theta}_2$
$C_{l\beta}$	-0.0255	-0.0194	-0.0232	$C_{n\delta_a}$	-0.0088	-0.0031	-0.0083
C_{lp}	-0.3817	-0.2967	-0.3403	$C_{n\delta_r}$	-0.0996	-0.0938	-0.0978
C_{lr}	0.0504	0.0421	0.0472	C_{D0}	0.0526	0.0620	0.0526
$C_{l\delta_a}$	0.3490	0.2762	0.3150	$C_{D\alpha}$	-0.0863	-0.0741	-0.0835
$C_{l\delta_r}$	0.0154	0.0112	0.0140	$C_{Y\beta}$	-0.3462	-0.3589	-0.3949
C_{m0}	-0.0018	-0.0017	-0.0015	C_{Yp}	0.0073	0.0244	0.0140
$C_{m\alpha}$	-0.3701	-0.3495	-0.3931	C_{Yr}	0.2372	0.3137	0.2188
C_{mq}	-8.5026	-8.1499	-6.5773	$C_{Y\delta_r}$	0.1928	0.1897	0.1723
$C_{m\delta_e}$	-0.8778	-0.8382	-0.7974	C_{L0}	0.1470	0.0399	0.1461
$C_{n\beta}$	0.0954	0.0901	0.0942	$C_{L\alpha}$	4.5363	4.1394	4.5524
C_{np}	-0.0156	-0.0277	-0.0157	C_{Lq}	5.1515	8.5000	4.7409
C_{nr}	-0.1161	-0.0957	-0.0913	$C_{L\delta_e}$	0.3762	0.6132	0.5482

Using doublet signals as inputs, a comparison of the predicted responses was carried out using these two identified models. The graphs of the predicted response outputs of the two models are shown in Fig. 8, with the experimental test data shown in black, model $\hat{\theta}_1$ in blue, and model $\hat{\theta}_2$ in red. From the graphs it can be deduced that model $\hat{\theta}_2$ has a more robust and seamless prediction of the measured data.

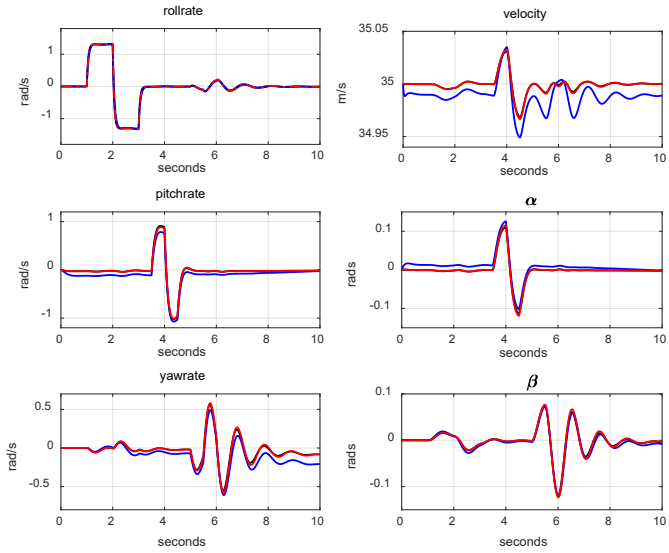

Figure 8
Comparison of model fit to measured outputs

Conclusion

A procedure for identification of an unmanned aerial vehicle aerodynamic parameters has been presented. The model parameter estimates extracted using the equation-error method were used as prior estimates for an extended approach in identification. Since the aerodynamic forces and moments depend linearly on the current values of states and controls, a linear time invariant aerodynamic model formulation was sought such that the deviations of the outputs from the test model could be extracted. The desired time history of inputs was computed using these deviations through an inverse simulation, and subsequently the force parameter estimates were updated using the output-error method. There were considerable asymptotic improvements in the model parameters leading to an improved model estimate which was evidenced in the force and moments model fits, and the response plots. The proposed identification procedure presented is simple and practical, and the results show an improved modelling performance.

References

[1] M. S. Roeser and N. Fezans. Method for Designing Multi-Input System Identification Signals Using a Compact Time-Frequency Representation. *CEAS Aeronautical Journal*, 12(2): 291-306, 2021 https://doi.org/10.1007/s13272-021-00499-6

[2] E. A. Morelli and J. A. Grauer. Practical Aspects of Frequency-Domain Approaches for Aircraft System Identification. *Journal of Aircraft*, 57(2): 1-25, 2020, https://doi.org/10.2514/1.c035599

[3] M. Mohamed. Parameter Identification of Flexible Aircraft Using Frequency Domain Output Error Approach. *IFAC Proceedings Volumes*,

47(1):1166-1171, 2014, https://doi.org/10.3182/20140313-3-IN-3024.00177

[4] E. A. Morelli. Multiple Input Design for Real-Time Parameter Estimation in the Frequency Domain. *IFAC Proceedings Volumes,* 36(16): 639-644, 2003, https://doi.org/10.1016/S1474-6670(17)34833-4

[5] J. A. Grauer. Frequency Response Estimation for Multiple Aircraft Control Loops Using Orthogonal Phase-Optimized Multisine Inputs. *Processes 2022,* 10(4): 619, https://doi.org/ 10.3390/pr10040619

[6] D. Ding, K. F. He, and W. Q. Qian. A Bayesian Adaptive Unscented Kalman Filter for Aircraft Parameter and Noise Estimation. *Journal of Sensors,* 2021, https://doi.org/10.1155/2021/9002643

[7] V. Klein and E. A. Morelli. *Aircraft System Identification Theory and Practice*, 2nd Edition, Sunflyte Enterprises, Virginia, 2016

[8] S. Subedi, B. Hosseini, J. Diepolder, and F. Holzapfel. Online Parameter Identification and Optimal Input Design Using Perturbed Nonlinear Programming. *Journal of Physics: Conference Series 2514*, 012020, 2023, https://doi.org/10.1088/1742-6596/2514/1/012020

[9] J. Shen, Y. Su, Q. Liang, and X. Zhu. Calculation and Identification of the Aerodynamic Parameters for Small-Scaled Fixed-Wing UAVs. *Sensors 2018,* 18(1): 206, https://doi.org/10.3390/s18010206

[10] M. S. Roeser, W. Mönnich, and M. Ritter. A Process for Time Domain Identification of a Flexible Aircraft Model from CFD/CSM Simulations. In *AIAA SciTech 2022 Forum,* San Diego, USA, 2022 https://doi.org/10.2514/6.2022-1303

[11] B. M. Simmons and P. C. Murphy. Wind Tunnel-Based Aerodynamic Model Identification for a Tilt-Wing, Distributed Electric Propulsion Aircraft. In *AIAA Scitech 2021 Forum*, Virtual Event, 2021, https://doi.org/10.2514/6.2021-1298

[12] B. M. Simmons. System Identification Approach for eVTOL Aircraft Demonstrated Using Simulated Flight Data. *Journal of Aircraft,* 60(4): 1078-1093, 2023, https://doi.org/10.2514/1.C036896

[13] L. Wang, R. Zhao, and Y. Zhang. Aircraft Lateral-Directional Aerodynamic Parameter Identification and Solution Method Using Segmented Adaptation of Identification Model and Flight Test Data. *Aerospace 2022,* 9(8): 433, https://doi.org/10.3390/aerospace9080433

[14] Q. Wang, F. Zheng, W. Qian, and D. Ding. A Practical Filter Error Method for Aerodynamic Parameter Estimation of Aircraft in Turbulence. *Chinese Journal of Aeronautics,* 36(2): 17-28, 2023 https://doi.org/10.1016/j.cja.2022.05.008

[15] L. C. S. Góes, E. M. Hemerly, B. C. O. Maciel, W. R. Neto, C. B. Mendonca, and J. Hoff. Aircraft Parameter Estimation Using Output-Error

Methods. *Inverse Problems in Science and Engineering,* 14(6): 651-664, 2006, https://doi.org/10.1080/17415970600573544

[16] J. Harris, F. Arthurs, J. V. Henrickson, and J. Valasek. Aircraft System Identification Using Artificial Neural Networks with Flight Test Data. In *International Conference on Unmanned Aircraft Systems (ICUAS),* Arlington, USA, 2016, https://doi.org/10.1109/ICUAS.2016.7502624

[17] T. J. J. Lombaerts, Q. P. Chu, J. A. Mulder, and D. A. Joosten. Modular Flight Control Reconfiguration Design and Simulation. *Control Engineering Practice*, 19(6): 540-554, 2011 https://doi.org/10.1016/j.conengprac.2010.12.008

[18] R. W. Beard and T. W. McLain. *Small Unmanned Aircraft; Theory and Practice*, 2nd Edition, Princeton University Press, New Jersey, 2012

[19] R. V. Jategaonkar. *Flight Vehicle System Identification: A Time Domain Methodology*, 2nd Edition, American Institute of Aeronautics and Astronautics, Virginia, 2015

[20] S. Kimathi and B. Lantos. Robust Aerodynamic Parameter Estimation of Unmanned Aircraft Based on Two-step Identification. *Periodica Polytechnica Electrical Engineering and Computer Science,* 67(4): 394-402, 2023, https://doi.org/10.3311/PPee.21948

[21] A. M. Kamal, A. M. Bayoumy, and A. M. Elshabka. Modeling and Flight Simulation of Unmanned Aerial Vehicle Enhanced with Fine Tuning. *Aerospace Science and Technology,* 51: 106-117, 2016 https://doi.org/10.1016/j.ast.2016.01.022

[22] D. J. Murray-Smith. Feedback Methods for Inverse Simulation of Dynamic Models for Engineering Systems Applications. *Mathematical and Computer Modelling of Dynamical Systems,* 17 (5): 515-541, 2011 https://doi.org/10.1080/13873954.2011.584323